Unizik Journal of Technology, Production and Mechanical Systems (UJTPMS)

journal homepage: https://journals.unizik.edu.ng/index.php/ujtpms/about

Modelling of the drying characteristics of *Gmelina arborea* wood: kinetics and thermodynamics studies

Chinagorom Ajike[1*], Samuel Ogbonna Enibe[1], Ugochukwu C. Okonkwo[1], Amoo-Onidundu, O. N[2]

[1]Department of Mechanical Engineering, Nnamdi Azikiwe University, Awka 420218, Nigeria.
[2]Department of Forest Products Development and Utilization, Forestry Research Institute of Nigeria, Ibadan 200272, Nigeria.

ARTICLE INFO

Article history:
Received 27 April 2022
Revised 5 July 2022
Accepted 22 July 2022

Available online 30 July 2022

Keywords:
drying, moisture desorption isotherm, thin-layer kinetic model, *Gmelina arborea*.

ABSTRACT

The study carried out the modelling of the drying characteristics of *Gmelina arborea* wood sample (GmW) under the influence of various process variables such as drying time (0 - 40 h), temperature (45 – 75ºC) and airflow velocity (1.2 – 4.2 m/s). The moisture desorption isotherms, kinetics and thermodynamics studies of GmW were also investigated. The anatomical analysis result shows that the GmW sample has an average lumen size of 147.44 µm, which indicates a high moisture content. Based on the moisture desorption isotherm study, the Guggenheim, Anderson and de Boer (GAB) model, with the lower sum of squared error value (0.046) demonstrated the best fit to the experimental desorption data, while the Demir model emerged as the kinetics model of best fit. The average change in enthalpy (ΔH), change in entropy (ΔS) and Gibbs free energy (ΔG) values recorded in the study are 2515.86 kJ/mol, 334.2134 J/mol*K and 108778.5 kJ/mol, respectively. These thermodynamics parameters demonstrated that the heat and mass transfer coefficients varied linearly with temperature.

1. Introduction

Basic hygroscopicity is a fundamental characteristic that governs the handling, storage and application, of agricultural materials [1]. Timber, as an agricultural material, is a valued natural resource that serves directly as a material for use in construction, paper manufacturing, specialty wood products such as furniture, and as a fuel source [2]. Notably, the functional development of the tree from which the lumber is cut takes place in the presence of moisture, and the wood remains "green" or moist throughout the life of the tree. This moisture is present in freshly cut lumber, and for many reasons must largely be removed by seasoning to ease its transportation, improve its shelf life and make them suitable for many of its various uses.

In addition to the aforementioned benefits, drying timber is one method of adding value to sawn products from the primary wood processing industries. According to the Australian Forest and Wood Products Research and Development Corporation (FWPRDC), green sawn hardwood, which is sold at about $350 per cubic meter or less, increases in value to $2,000 per cubic meter or more with drying and processing. Prompt drying immediately after the felling of trees protects timber against primary decay, fungal stain and attack by certain kinds of insects. Thus, proper drying under controlled conditions before use is of great importance in the lumbering industry.

There are two methods of removing excess moisture from greenwood, namely, the natural method (air seasoning) and the artificial method (kiln seasoning) [3]. With developments and advancements in technology, the artificial method of controlled drying of wood has come to stay with the accompanying benefits. According to Ohagwu, et al [4], industrial kiln-drying techniques have been developed for wood drying, though with limited implementation and validation regarding the woods grown in Nigeria. Also, the practical application of these kilns by typical small and medium scale wood processing artisans (who form the bulk along the wood processing value chain) is largely undocumented.

Due to the complexity and multi-equilibrium nature of the drying process, numerous models with varying degrees of sophistication have been developed for their simulation. According to Onu, et al [5], the rate at which wood dries depends upon several factors, the most important of which are the temperature, the dimensions of the wood, and the relative humidity. Models are used to inform and optimize the design and control of process conditions [6]. Thin layer models describe the drying phenomena in a unified way, regardless of the controlling mechanism. They have been used to estimate the drying times of several products and to generalize drying curves. In the development of thin-layer drying models for agricultural products, generally, the moisture

*Corresponding author: chinagorom.ajike@fedcs.gov.ng

content of the material at any time after it has been subjected to constant relative humidity and temperature conditions is measured and correlated to the drying parameters [7]. Similarly, the relationship between water activity, moisture content, and temperature is captured in the moisture desorption isotherm. Moisture desorption is a complex and unique process due to the different ways of interaction between water and the solid components of the material at different moisture contents. Several models are applicable for the determination of the desorption isotherms for different materials.

The general desirability of GmW species in the Nigeria timber industry occasioned by the combined effects of its fast growth has been reported. Despite the fact that this specie is highly sought-after, an extensive literature survey portrayed the existence of few reports on its kinetics modelling and thermodynamics studies which hold great information on its large-scale drying application. Hence, this study tried to fill-up the identified knowledge gaps.

The aim of this research was to carry out the kinetics modelling and thermodynamics studies of the drying characteristics of *Gmelina arborea* wood.

2. Materials and Methods

2.1 Material collection and preparation

The pieces of unprocessed *Gmelina arborea* (GmW) used for the study were obtained from a local sawmill in the Edo State of Nigeria (Lat. 6.5438 ^{o}N and Long. 5.8987 ^{o}E). Categorization of the physical properties of the wood sample was achieved by visual inspection. The feel-and-touch approach was used to determine the wood grain texture composition.

2.2 Anatomical investigation

The GmW samples of 0.01 m x 0.01 m were obtained and boiled in water for 2 h for softening and to drive out trapped air. The sample was then cut into the transverse, radial and longitudinal sections (using the Reichert sliding microtome, model 843-02 G) and afterwards washed in distilled. Sections of the sample were stained in safranin for 2 min in readiness for efficient microscopic study and then washed using distilled water to remove the safranin stains. After washing, the sections were tinkered with by dipping them into different ethanol concentrations (5 % to 50 %) to reduce the risk of damage. Thereafter, the wood sections were covered with clove oil for 1 h to remove any residual trace of ethanol from the specimen. Using filter paper, the excess clove oil was removed from the sample before mounting them (samples) on a slide. Slight Canada balsam, a mounting medium was added for preservation and the slide was covered again with glass. Colouring materials that could adversely affect visibility under the microscope were bleached off by dipping the specimen in 5 % sodium hydroxide (NaOH) for about 30 min. The specimen was later soaked in sodium hypochlorite (NaOCl) for 24 h and rinsed severally in water, while air bubbles were removed by gentle application of heat. Afterwards, a coloured photomicrograph of the sample was taken using the digital camera mounted on the Reichert light microscope. The descriptive terminologies, measurements and microscopic features for hardwood identification outlined above are all in line with Cooper, et al [8] and Angyalossy-Alfonso, et al [9].

2.3 Wood seasoning experimentation

The freshly sawn GmW sample of 0.5 m x 0.25 m x 0.0254 m, in length, width and thickness, respectively, were loaded in the laboratory-scale wood drying machine (LSWDM). The device was fabricated using a stainless-steel sheet and insulated from the environment with a 0.0254 m loose-fill thermal fiberglass insulator. The specified number of wood samples (about 10 samples of the aforementioned dimension per batch) were piled into the LSWDM while leaving about a 0.0254 m separation gap to ensure even and adequate circulation of air. The system was operated on a closed-loop basis, with a unidirectional airflow from the fan.

The incoming air was preheated using an electric 0.6 kW heater at the inlet duct and the heater power-control unit was used to adjust air temperature. The temperature inside the drying chamber was continuously monitored using a thermocouple (type K, ±1 ^{o}C) that was embedded in the control component. Air was directed through a series of electrical resistance heaters to reach higher temperatures and was then redirected towards the drying chamber. The drying air flows horizontally over the samples. A blower creating axial flow and a module for controlling its rotation speed was used to adjust air velocity. A digital hot wire anemometer (TESTO 425, ±0.03 m/s, made in Germany) was used to measure the air velocity. The range of airflow velocity used is between 1.2 – 4.2 m/s and the air temperature was varied between 45 ^{o}C and 75 ^{o}C. The value range of the air temperature and airflow velocity were selected based on the available research literature on industrial air-drying applications.

Before each experiment, the dryer was left idle for about 30 min to provide attain a steady state based on predetermined experimental drying conditions. Then, a specific mass of the GmW samples was stacked uniformly in a thin layer on a perforated tray within the LSWDM. The moisture content (MC) reduction was recorded periodically (between 5 – 40 h). Consequently, the drying process was terminated once the samples' MC reached equilibrium moisture content (EMC). To foreclose experimental error, all the drying experiments were conducted in triplicates and their mean value was subsequently adopted.

2.4 Measurement of relevant drying parameters

The moisture content (MC) of the GmW sample on a dry basis was conducted following the standard procedure documented by the American Society for Testing and Materials standard method (ASTM D2974-14) [10]. The final moisture content at a given time is evaluated from Eq. (1). Similarly, the dimensionless moisture ratio (MR) and the water activity (a_w) value

(which measures the extent to which inherent moisture content can get involved in physical and chemical deteriorative reactions) is evaluated from Eqs. (2) and (3), respectively.

$$\%MC = \frac{w_2}{w_1} * 100 \quad (1)$$

$$MR = \frac{M_t - M_e}{M_0 - M_e} \quad (2)$$

$$a_w = \frac{\%RH}{100} \quad (3)$$

Where w_2 and w_1 are the post and pre-drying weight of the GmW sample. RH is the relative humidity, while M_t, M_o, and M_e are moisture contents (MC) at any instant of time, initial MC and equilibrium MC, respectively.

2.5 Mathematical modelling

The GmW drying data were fitted into five (5) thin-layer drying models and five (5) moisture desorption isotherm models. The theoretical background of the models has been extensively discussed elsewhere [11, 12], while the mathematical expression of the models is presented in Tables 1 and 2, respectively. The experimental data were modelled using the SOLVER function of the Microsoft Excel software 2016 (Microsoft Corporation, Redmond, Washington, USA). The goodness of the respective model fit was ascertained from the values of coefficient of determination (R^2) and the sum of squared error (SSE) values. According to Shi, et al [13], the higher the R^2-values and the lower the SSE values the better the model fitting. The R^2 and SSE values were determined using Eqs. (4) and (5), respectively [14].

$$R^2 = \frac{\sum_{i=1}^{N}(MR_i - MR_{pre,i}) \cdot \sum_{i=1}^{N}(MR_i - MR_{exp,i})}{\sqrt{\left[\sum_{i=1}^{N}(MR_i - MR_{pre,i})^2\right] \cdot \left[\sum_{i=1}^{N}(MR_i - MR_{exp,i})^2\right]}} \quad (4)$$

$$SSE = \frac{1}{N}\sum_{i=1}^{N}\left(MR_i - MR_{pre}\right)^2 \quad (5)$$

Table 1 - Kinetics models adopted in the study

Model names	Model equation
Geometric [15]	$MR = a_G t^{-n}$
Vega-Lemus [16]	$MR = (a_V + k_V t)^2$
Logarithmic [17]	$MR = a_L * \exp(-k_L t) + c_L$
Parabolic [18]	$MR = a_P + b_P t + c_P t^2$
Henderson-Pabis [19]	$MR = a_H * \exp(-k_H t)$
Demir *et al.* [20]	$MR = a_D * \exp(-k_D t)^n + b_D$
Midilli [21]	$MR = a_M * \exp(-k_M t) + b_M t$

MR = Moisture ratio

Table 2 - Moisture desorption isotherm models adopted in the study

Model	*Model equation*
BET [22]	$EMC = \frac{x_m * C_B * a_w}{(1 - a_w) * (1 - a_w + C_B a_w)}$
GAB [23]	$EMC = \frac{x_m + k\frac{c_G}{T}a_w}{(1 - k_G a_w)\left(1 - k_G a_w + \frac{c_G}{T}k_G a_w\right)}$
Henderson [24]	$EMC = \left(-\frac{ln(1 - a_w)}{c_{He}}\right)^{\frac{1}{n_h}}$
Halsey [25]	$EMC = \left[-\frac{exp(A_{Ha} + B_{Ha}T)}{ln\, a_w}\right]^{\frac{1}{C}}$
Oswin [26]	$EMC = C_O\left[\frac{a_w}{1 - a_w}\right]^{n_o}$

EMC = equilibrium moisture content; a_w = experimentally derived water activity; and T = temperature

2.6 Determination of the thermodynamic parameters

The knowledge of the effective moisture diffusivity (D_{eff}) of a given drying operation is indispensable for determining the relevant thermodynamic parameter. Fick's diffusion equation for particles with slab geometry is used to calculate the effective moisture diffusivity. Therefore, Fick's equation for describing effective moisture diffusivity is generally expressed as Eq. (6).

$$MR = \frac{M-M_e}{M_0-M_e} = \frac{8}{\pi^2}\sum_{n-1}^{\infty}\frac{1}{(2n-1)^2}\exp\left(\frac{-D_{eff}(2n-1)^2\pi^2 t}{4L^2}\right) \quad (6)$$

Where 'n' is the number of terms taken into consideration, 't' is the drying time (s), 'D_{eff}' is effective moisture diffusivity (m2/s) and 'L' is the average thickness of the sample (m). After considering the first term of Eq. (6) for a long drying period, Kingsly, et al [27] reported a simplification of Eq. (6) to Eq. (7). Upon linearization, Eq. (7) becomes Eq. (8).

$$MR = \left(\frac{8}{\pi^2}\right)\exp\left(\frac{\pi^2 D_{eff} t}{4L^2}\right) \quad (7)$$

$$\ln(MR) = \ln\left(\frac{M-M_e}{M_0-M_e}\right) = \ln\left(\frac{8}{\pi^2}\right) - \left(\frac{D_{eff}\pi^2 t}{4L^2}\right) \quad (8)$$

Furthermore, the different thermodynamics properties can be determined such as enthalpy (ΔH), entropy (ΔS) and Gibbs free energy (ΔG) according to Eqs. (9) – (11).

$$\Delta H = E_a - RT \quad (9)$$

$$\Delta S = R\left[\ln k - \ln\left(\frac{k_b}{k_h}\right) - \ln T\right] \quad (10)$$

$$\Delta G = \Delta H - T\Delta S \quad (11)$$

Where k_b and k_h are Boltzmann (m^2 $kg.s^{-2}$ K^{-1}) and Planck's constant (J. s), respectively.

3. Results and Discussion

3.1 Wood sample characterization

According to the experimental findings, the GmW is a fast-growing wood species that has a medium-coarse texture, pale yellow colour and is lustrous when freshly sawn. The tissue dimension of the sample is shown in Table 3. From the data presented, an average lumen size of 147.44 µm was recorded. Notably, the lumen holds a majority of the available water in a wood sample and the relatively large lumen size obtained in the study indicates the presence of high moisture content in the GmW sample. A proper understanding of the ray formation in wood anatomy is important because it has been established that common wood drying defects tend to occur along with the rays. The tangential and transverse photomicrograph of the GmW sample is presented in Figure 1 (a and b), respectively. According to the photomicrograph, the GmW sample has a multi-seriate ray arrangement, hence the sample is more prone to wood drying defects when poorly processed during drying when compared to di-seriate wood samples.

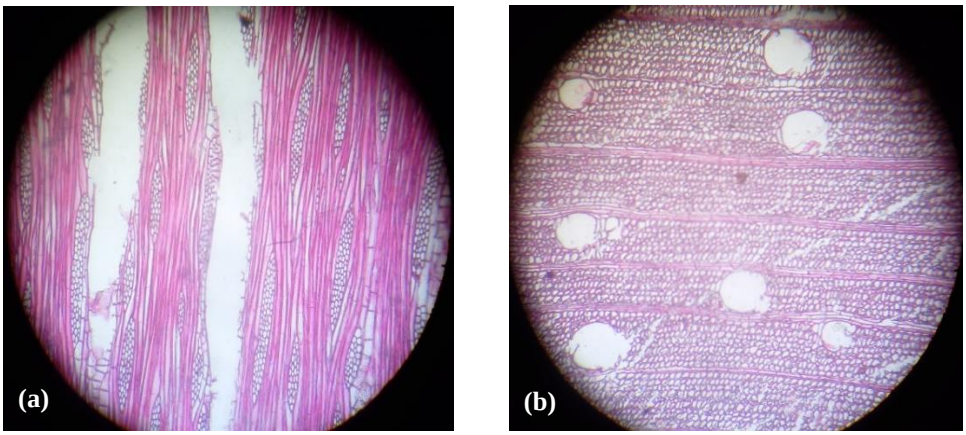

Fig. 1 - Photomicrograph of the (a) tangential (b) transverse section of the GmW sample (Mag. x100)

Table 3 - Tissue dimensions of selected wood species

Lumen size (µm)	Fibre length (µm)	Fibre diameter (µm)	Density (kg/m^3)	Ray width
147.44	790	165	510	Multi-seriate

3.2 Effect of process variables

3.2.1 Effect of drying time on wood drying

Figure 2 shows the effect of drying time (h) on moisture content reduction (%) for the GmW sample. As shown in Figure, the drying time varied by an interval of 5 h from 0 to 40 h, and with an initial moisture content of 90 % at zero (0) h, an increase in the drying time (from 0 to 30 h) generally caused a corresponding increase in the percentage of moisture loss. Beyond 30 h, a negligible moisture content reduction was recorded, hence the equilibrium moisture content (EMC) was achieved at the drying time of 30 h. Furthermore, upon close observation of the plotline of Figure 2, it was deduced that within the first 5 h of drying, rapid moisture loss was recorded which culminates in about 55 % reduction in the initial moisture content. A rapid loss of the free waters which are loosely held to the wood sample explains the observed initial rapid moisture loss [16]. Meanwhile, within the second 5 h of drying (that is after drying for 10 h), the previously observed rapid moisture content loss was no longer the case. Incidentally, only about 5.6 % of moisture content was lost from the sample. As expected, the % moisture loss decreased as the duration of drying extended. This is because the moisture content remaining in the wood samples sequel to the initial rapid loss of the free waters are now bound more and more strongly to the interior of the wood. The % moisture content loss from the samples further diminished as the drying time extended beyond 10 h. As seen in Figure 2, only a minimal % moisture loss of 7.09% was recorded within the next 20 h (that is from 10 h to 30 h) of drying. This is because the % moisture content within the wood interior at this point is bound by very strong chemical bonds. Hence, moisture escapes more slowly even at a relatively high operating temperature of 70^0C.

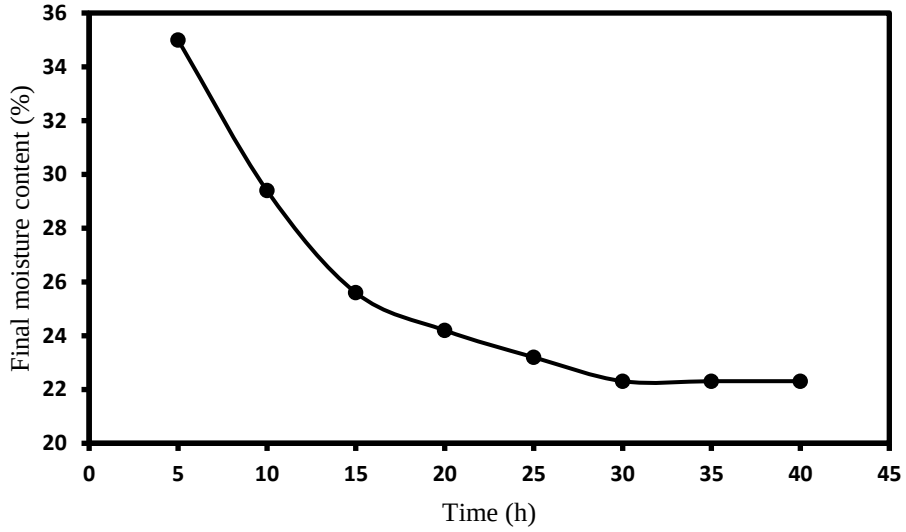

Fig. 2 - Plot of the effect of time on the final moisture content [Air velocity = 4.2 m/s, Temp = 70 ^{0}C]

3.2.2 Effect of air velocity on wood drying

For efficient and effective drying of moisture-laden material, uniform air movement over the surface of such material is essential [29]. This is because effective airflow is relevant for two reasons; for transferring heat energy sufficient to evaporate the moisture and to carry away the vaporized moisture from the wood surface. The graphical representation of the relationship between air velocity and % moisture content is presented in Figure 3. It was observed that at the optimum drying time of 30 h, there existed a consistent decrease in % moisture content with an increase in the air velocity, from 1.2 to 4.2 m/s.

At an air velocity of 1.2 m/s a final moisture content of 24.01 % was recorded, thus translating to about 65.99 % moisture loss from the initial moisture content of 90 %. Similarly, with a further increase in the air velocity (up to 4.2 m/s), a consistent increase in % moisture loss (decrease in final moisture content) was recorded. This observed decreasing final moisture content with a decrease in air velocity (from 4.2 to 1.2 m/s) could be explained thus. The movement of air across wet surfaces are accompanied by a drop in the air temperature and a corresponding rise in the air humidity. This temperature drops and rise in relative humidity is a function of the volume of airflow. Therefore, at low air velocity, there is limited airflow across the wet surface; thus, resulting in a quick rise in the relative humidity of the air, with an attendant drop in the air temperature. When this is the case, a low % moisture content loss will be recorded as rightly observed in the study [29]. Similarly, the increase in air velocity (from 1.2 to 4.2 m/s), causes an increased airflow volume through the surface and interstitial space of the sample. This increase in airflow implies more airflow across the surface of the wood samples, thus a smaller temperature drop and a smaller relative humidity rise.

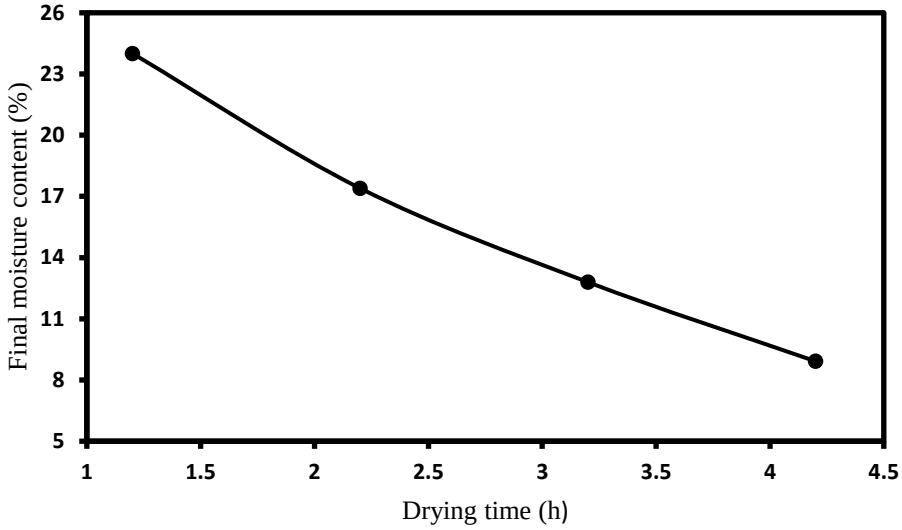

Fig. 3 - Plot of the effect of airflow velocity on the final moisture content [Time = 30h, Temp = 70 ^{0}C]

3.3 Drying process modelling

3.3.1 Modelling of moisture desorption isotherm

The desorption equilibrium moisture relationship is important for the determination of the lowest attainable moisture content at constant temperature and pressure [30]. In this work, five (5) mathematical models were used to describe the desorption isotherm. Meanwhile, due to the inadequacy of the coefficient of determination as adjuring criteria for selecting the model of best fit in nonlinear regression, the sum of the square error model was adopted. Hence, the lower the SSE value for a given desorption isotherm model, the better the model fit [31, 32].

From the data presented in Table 4, the GAB model emerged as the best fit with the lowest SSE value of 0.046. Furthermore, the model's R2 value is unity, thus indicating that 100 % of the observed variation in the drying data could be explained by the model. Having identified the best fit model, there is the need to relate the models' theoretical background to the current moisture desorption system. Accordingly, the GAB model is a blend of Langmuir and BET isotherm models and describes the classical mono-molecular layer expression in Langmuir's adsorption isotherms and the multilayer adsorption corresponding to Raoult's law. It describes most of the temperature effects on isotherms using Arrhenius type equations. GAB model postulates that the state of sorbate water molecules in the second adsorption layer is identical to the one in the superior layers, but different from those of the pure liquid state. With the incorporation of a third parametric constant 'k' to the isotherm equation, the differences in the chemical potential standard between the trapped water molecules on the wood material and those of the pure liquid state could be effectively accounted for.

To further validate the best fit models, the experimentally derived equilibrium moisture content was compared with the predicted data sets generated by the different models as shown in Figure 4. Halsey, Oswin, BET and Henderson models emerged as the second, third, fourth and fifth best-fit model for GmW, with SSE values of 14.66, 33.98, 38.45 and 51.11 respectively. Further observation of (Table 4), showed that the SSE (14.66) values for Halsey (second best-fit) model was about three hundred and eighteen (318) times greater than those recorded for the GAB model. Equally, the SSE values for Oswin, BET and Henderson models progressively increased indicating higher sum of squared errors. This observation elucidates the fact that even though the Halsey model emerged as the second best-fit, the fitting ability is no way near that of GAB model. Upon visual inspection, a close correlation was observed between the experimental and GAB plotlines, thereby confirming the validity of the emergence of the GAB model as the best fit.

Table 4 - Isotherm parameters and corresponding goodness-of-fit test values

BET	GAB	Henderson	Halsey	Oswin
M_0 = 22.80	k_G = 14.16	C_H = 0.056	A = 4.44	C_O = 67.96
C_B = 27.85	x_G = 8.86	n_H = 0.067	B = -0.03	n_O = 0.54
R^2 = 0.99	C_G = 5.60	R^2 = 0.99	C = 0.37	R^2 = 0.99
SSE = 38.45	R^2 =1.00	SSE = 51.11	R^2 = 0.99	SSE = 33.98
	SSE = 0.046		SSE = 14.66	

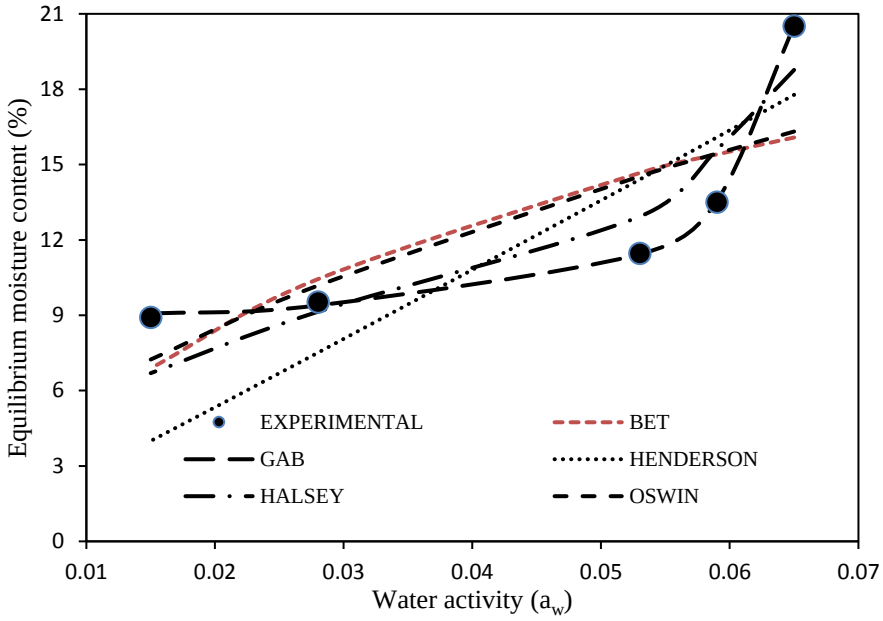

Fig. 4 - Plot of the predicted and experimentally derived equilibrium moisture content

3.3.2 Modelling of wood drying kinetics

Thin-layer drying equations constitute an important tool in the mathematical modelling of various materials drying. This is because they describe the drying phenomena in a unified way, regardless of the controlled mechanism, and they have found wide applications due to their ease of use. In this study, five (5) thin-layer models were employed to describe the drying kinetics of the GmW sample. As already explained in section 3.3.1, the respective models' consistency and fitting adequacy was informed by their SSE values. Based on all goodness-of-fit test criteria (R^2 and SSE values), the top three superior and perfect fitting of the experimental data were observed employing Demir et al, logarithmic and Henderson-P models, respectively (Table 5). Considering the theory behind the top three best-fitting models with regards to all the adjuring criteria (highest R^2 value and lowest SSE values); the Henderson-P model supposes that the moisture particles are homogenous and isotropic. The model also assumes that these moisture particles have negligible pressure variation during their transport from the interior layer of the wood material. The Demir et al model postulates that the initial moisture content of the wood material is independent of other variables; thus, moisture equilibrium is assumed to occur at the wood-air interface during the drying operation. The logarithmic model assumes that the temperature distribution within the wood material is uniform and equal at air temperature; thus, the effective moisture diffusivity is constant.

However, the selection of Demir et al., Logarithmic and Henderson-P as the top three best-fitting models for GmW, do not in any way suggest that Midilli-Kucuk, and Parabolic models should be considered as poor-fitting models. In fact, with regards to the criteria for adjuring best fit models (high correlation coefficient, R2 and low error value, SSE), it could be concluded that Midilli-Kucuk, and Parabolic models also showed good fitting of the experimental kinetics data for GmW, returning SSE values of 6.3E-03 and 1.4E-04 respectively.

To further evaluate the accuracy and consistency of the various models in parameter prediction, curve fitting was applied. This helps in describing the correlation between the model predicted MR data sets and experimental MR data sets. The predicted data points generated by the various models Henderson-P, Demir et al and Logarithmic models were plotted alongside the experimental data points as shown in Figure 5. The better the correlation between the data points of a given model with the experimental data points, the more accurate the model description becomes. By visual inspection, the plotlines of Demir et al, Logarithmic and Henderson-P models showed greater correlation with the experimental data points. Such observation validates the emergence of these models as the all-time top three (3) models for describing the drying kinetics of GmW.

Table 5 - Kinetic parameter and corresponding goodness-of-fit test values

Henderson-Pabis	Midilli-Kucuk	Logarithmic	Demir et al	Parabolic
a_H = 0.36	a_M = 2.03	a_L = 0.35	a_D = 0.35	a_P = 0.27
k_H = 0.13	b_M = 1.7E-03	k_L = 0.12	b_D = -5.4E-03	b_P = -0.02
R^2 = 0.99	K_M = 0.47	c_L = -5.4E-03	k_D = 0.35	c_P = 4.1E-04
SSE = 4.6E-05	R^2 = 0.99	R^2 = 0.99	n_D = 0.35	R^2 = 0.99
	SSE = 6.3E-03	SSE = 3.7E-05	R^2 = 0.99	SSE = 1.4E-04
			SSE = 3.7E-05	

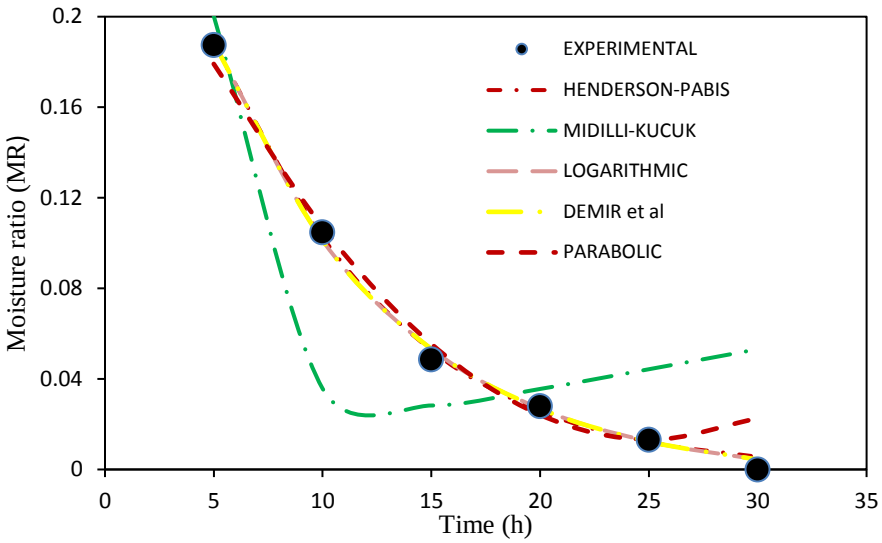

Fig. 5 - Plot of the predicted and experimental moisture ratios

3.4 Thermodynamics

The study of the thermodynamic properties of a system is important in the design of drying equipment, for evaluating the drying process kinetics and modelling. Generally, the thermodynamic study approach assumes that the heat of desorption of the bound water inherent in the wood sample depends on the moisture content state, the superficial layer energy state, and the environmental properties [33]. The thermodynamic parameters (the enthalpy change, ΔH, entropy change, ΔS and Gibbs free energy, ΔG) values for GmW were calculated from the desorption data and presented in Table 6. For effective discussion of the subject matter, the different thermodynamic properties will be accorded independent considerations further down the sections.

3.4.1 Enthalpy change (ΔH)

Usually, the value of ΔH is a useful indicator for elucidating the water-wood bond strength. It is also related to the quantity of energy released and the available free pressure accompanying the drying operation [33, 34, 35]. The ΔH values shown in Table 5 were negative at all temperatures. However, these values became increasingly negative with a temperature increase from 323 to 343 K. Theoretically, the negative sign convention depicted by the ΔH values is expected considering the temperature dependence of ΔH. It is a well-known fact that the breakage of the intermolecular bond between the water molecules and the wood, as well as the subsequent diffusion of those water molecules to the drying surface, requires sufficient energy. Thus, the progressive decrease in the ΔH values suggests that with temperature increase, the energy required for the drying operation is reduced [36,37,38], while studying the variation of the physical properties of soybeans during cooking, also observed similar behaviour.

3.4.2 Entropy change (ΔS)

The values of ΔS are related to the degree of disorderliness within the wood sample. As shown in Table 6, the ΔS values were negative and also vary linearly with temperature. As was the case with ΔH, the ΔS values became increasingly negative as the temperature increased from 323 to 343 K. In this case, the negative sign convention is attributed to the existence of chemical desorption and/or structural alterations of the sample; hence, the drying processes are considered to be entropically unfavourable. Similarly, Corrêa, et al [39] reported that the decrease in ΔS-values with temperature increment can be explained by the fact that when the product is being dehydrated, moisture content decreases and the movement of water molecules become more restricted, thereby limiting the number of available sites. Bayram, et al [37], while studying the variations of the physical properties of soybeans during cooking, observed positive values for entropy changes.

3.4.3 Gibbs Free Energy (ΔG)

ΔG is related to the energy required to ensure the availability of sorption sites [40]. According to the values depicted in Table 6, ΔG-values were positive, an indication that the drying process in this study is non-spontaneous, as the wood samples often possess high moisture content at harvest. This trend of result characterizes an endergonic reaction, where energy is supplied from the external to induce the spontaneity of the reaction. Expectedly, this observation is not surprising, since Nkolo, et al [40] and Okonkwo, et al [41] opined that drying is a non-spontaneous process. Meanwhile, Corrêa, et al [42] attributed the magnitude of ΔG values to the amount of work required to create available desorption sites. In Table 6, the magnitude of ΔG values was in the range of 105 kJ/mol, thus suggesting that substantive work was put into the creation of active desorption sites on GmW. Oliveira, et al [36], Corrêa, et al [42] and Martins, et al [43] obtained similar values for strawberry, coffee cherry and timbó leaf drying studies, respectively.

Table 6 - Thermodynamic properties showing ΔH, ΔS and ΔG

Temp (K)	+ΔG (kJ/mol)	-ΔH (kJ/mol)	-ΔS (J/mol*K)
323	105437.0	2432.72	333.962
328	107107.1	2474.29	334.090
333	108777.9	2515.86	334.215
338	110449.3	2557.43	334.339
343	112121.3	2599.00	334.461

4. Conclusions

This study carried out the modelling of the drying characteristics of GmW. The anatomical features of GmW show distinct and unique differences and further confirm the complex relationship and interactions observed in the drying process parameters. It was generally observed that the percentage moisture loss decreased as the duration of drying extended, with the establishment of the optimum drying condition at 30 h. Also, a consistent decrease in percentage moisture content was observed for all the wood samples as the air velocity increased from 1.2 to 4.2 m/s, while the increase in temperature caused a corresponding increase in the percentage moisture content loss. The GAB and Henderson-Pabis models emerged as the best fit for the experimental moisture desorption and thin-layer kinetic data for GmW. Equally, thermodynamics studies showed a consistent decrease in the ΔH and ΔS values with temperature increase, while ΔG values increased with the elevation of drying temperature. The positive ΔG values indicate the non-spontaneity of the drying process.

NOMENCLATURE

a_w	Water activity
ΔG	Gibbs free energy
ΔH	Enthalpy change
ΔS	Entropy change
D_{eff}	Effective diffusivity (m^2/s)
D_0	Pre-exponential factor of the equation (m2/s)
k_b	Boltzman constant (m^2 $kg.s^{-2}$ K^{-1})
k_h	Planck's constant (J. s)
MR_{exp}	Experimentally derived moisture ratio
MR_i	ith value of the moisture ratio to be predicted
MR_{pre}	Model predicted moisture ratio
R^2	Coefficient of determination
t	Time (s)
T	Absolute air temperature (K)

LIST OF ABBREVIATIONS

BET	Brunauer-Emmett-Teller
EMC	Equilibrium moisture content
GAB	Guggenheim, Anderson and de Boer
GmW	*Gmelina arborea* wood
LSWDM	Laboratory scale wood drying machine
MC	Moisture content
MR	Moisture ratio
SSE	Sum of squared error

References

[1] Aviara, N.A., Moisture sorption isotherms and isotherm model performance evaluation for food and agricultural products. Sorption in 2020s, 2020: p. 143.

[2] Khouya, A., Performance assessment of a heat pump and a concentrated photovoltaic thermal system during the wood drying process. Applied Thermal Engineering, 2020. 180: p. 115923.

[3] Okigbo, L., Sawmill industry in Nigeria. Sawmill industry in Nigeria., 1964.

[4] Ohagwu, C. and B. Ugwuishiwu, Status of wood processing and storage in Nigeria. Nigerian Journal of Technology, 2011. 30(2): p. 94-104.

[5] Onu, C.E., P.K. Igbokwe, J.T. Nwabanne, C.O. Nwajinka, and P.E. Ohale, Evaluation of optimization techniques in predicting optimum moisture content reduction in drying potato slices. Artificial intelligence in Agriculture, 2020. 4: p. 39-47.

[6] Druzgalski, C. L., A. Ashby, G. Guss, W. E. King, Tien T. Roehling, and Manyalibo J. Matthews. "Process optimization of complex geometries using feed forward control for laser powder bed fusion additive manufacturing." Additive Manufacturing 34 (2020): 101169.

[7] Afolabi, T & Agarry, Samuel. (2014). Mathematical Modelling and Simulation of the Mass and Heat Transfer of Batch Convective Air Drying of Tropical Fruits. 23. 9-18.
[8] Cooper, L., R.L. Walls, J. Elser, M.A. Gandolfo, D.W. Stevenson, B. Smith, J. Preece, B. Athreya, C.J. Mungall, and S. Rensing, The plant ontology as a tool for comparative plant anatomy and genomic analyses. Plant and Cell Physiology, 2013. 54(2): p. e1-e1.
[9] Angyalossy-Alfonso, V., P. Baas, S. Carlquist, J. Peres-Chimelo, V. Rauber-Coradin, P. Détienne, P. Gasson, D. Grosser, J. Ilic, and K. Kuroda, List of microscopic features for hardwood identification. International Association of Wood Anatomists Bulletin, New Series, 1989. 10: p. 219-332.
[10] ASTM, D., Standard test methods for moisture, ash, and organic matter of peat and other organic soils. D2974-07, 2007.
[11] Midilli, A. and H. Kucuk, Mathematical modeling of thin layer drying of pistachio by using solar energy. Energy conversion and Management, 2003. 44(7): p. 1111-1122.
[12] Gichau AW, Okoth JK, Makokha A., Moisture sorption isotherm and shelf-life prediction of complementary food based on amaranth-sorghum grains. J Food Sci Technol. 2020;57(3):962-970. doi:10.1007/s13197-019-04129-2
[13] Shi, Q., Y. Zheng, and Y. Zhao, Mathematical modeling on thin-layer heat pump drying of yacon (Smallanthus sonchifolius) slices. Energy Conversion and Management, 2013. 71: p. 208-216.
[14] Dinani, S.T., N. Hamdami, M. Shahedi, and M. Havet, Mathematical modeling of hot air/electrohydrodynamic (EHD) drying kinetics of mushroom slices. Energy Conversion and Management, 2014. 86: p. 70-80.
[15] Hacihafizoğlu, Oktay & Cihan, Ahmet & Kahveci, Kamil & Lima, Antonio. (2007). A liquid diffusion model for thin-layer drying of rough rice. European Food Research and Technology. 226. 787-793. 10.1007/s00217-007-0593-0.
[16] Guiné, R. (2010). Analysis of the drying kinetics of S. Bartolomeu pears for different drying systems. E-Journal of Environmental, Agricultural and Food Chemistry, 1772-1783.
[17] Chandra, P. K., and Singh, R. P., Applied Numerical Methods for Food and Agricultural Engineers. Boca Raton: CRC Press, 1995.
[18] Shittu, T.A., and Raji, A.O., Thin layer drying of African breadfruit (Treculia africana) seeds: modeling and rehydration capacity. Food and Bioprocess Technology, 2011. 4 : 224-231.
[19] Henderson S.M, Pabis S., Temperature effects on drying coefficients. J. Agric. Eng. Res., 1961. 6:169–174.
[20] Demir, V., Gunhan, T., and Yagcioglu, A. K., Mathematical modeling of convection drying of green table olives. Biosystems Engineering, 2007. 98, 47-53.
[21] Midilli, A., H. Kucuk, and Z. Yapar, A new model for single-layer drying. Drying technology, 2002. 20(7): p. 1503-1513.
[22] Brunauer, S., Emmett, P. H., & Teller, E., Adsorption of gases in multimolecular layers. Journal of the American Chemical Society, 1938. 60(1), 309-319. doi: 10.1021/ja01269a023.
[23] Guggenheim, E.A., Applications of Statistical Mechanics. Clarendon Press, Oxford. 1966.
[24] Henderson, S. M., A basic concept of equilibrium moisture. Transactions of the American Society of Agricultural Engineers, 1954. 33, 29-32.
[25] Halsey, G., Physical Adsorptionon Non-Uniformsurfaces. Journal of Chemistry and Physics, 1948. 16:931–37.
[26] Oswin, C. R., The Kinetics of Package Life III. The Isotherm. Journal of Chemical Industry, 1946. 65:419–421.
[27] Kingsly, R.P., R.K. Goyal, M.R. Manikantan, and S.M. Ilyas, Effects of pretreatments and drying air temperature on drying behaviour of peach slice. International journal of food science & technology, 2007. 42(1): p. 65-69.
[28] Gezici-Koç, Ö., S.J. Erich, H.P. Huinink, L.G. Van der Ven, and O.C. Adan, Bound and free water distribution in wood during water uptake and drying as measured by 1D magnetic resonance imaging. Cellulose, 2017. 24(2): p. 535-553.
[29] Mills, D., Pneumatic conveying design guide. 2003: Elsevier.
[30] Yu, Yong & Jiang, Xiuping & Ramaswamy, Hosahalli & Zhu, Songming & Li, Huanhuan, Effect of High-pressure Densification on Moisture Sorption Properties of Paulownia Wood. BioResources, 2018. 13. 2473-2486. 10.15376/biores.13.2.2473-2486.
[31] Mohamed, L.A., C.O. Aniagor, and A. Hashem, Isotherms and kinetic modelling of mycoremediation of hexavalent chromium contaminated wastewater. Cleaner Engineering and Technology, 2021. 4: p. 100192.
[32] Hashem, A., C. Aniagor, D. Hussein, and S. Farag, Application of novel butane-1, 4-dioic acid-functionalized cellulosic biosorbent for aqueous cobalt ion sequestration. Cellulose, 2021: p. 1-17.
[33] Ascheri, D.P.R., W.d.S. Moura, J.L.R. Ascheri, and E.A. Freitas Junior, Propriedades termodinâmicas de adsorção de água do amido de rizomas do lírio-do-brejo (Hedychium coronarium). Food Science and Technology, 2009. 29: p. 454-462.
[34] Gunathilake, Champathi & Senanayaka, D. & Adiletta, Giuseppina & Senadeera, Wiji, Drying of Agricultural Crops, 2018. 10.1201/9781351132398-14.
[35] Okonkwo U. C., Onokwai A. O., Okeke C. L., Osueke C. O. (2019). Investigation of the Effect of Temperature on the Rate of Drying Moisture and Cyanide Contents of Cassava Chips Using Oven Drying Process. International Journal of Mechanical Engineering and Technology (IJMET). 10(1) 1507-1520.
[36] Oliveira, G.H.H.d., D.M.S. Aragão, A.P.L.R.d. Oliveira, M.G. Silva, and A.C.A. Gusmão, Modelagem e propriedades termodinâmicas na secagem de morangos. Brazilian Journal of Food Technology, 2015. 18: p. 314-321.
[37] Bayram, M., A. Kaya, and M.D. Öner, Changes in properties of soaking water during production of soy-bulgur. Journal of Food Engineering, 2004. 61(2): p. 221-230.
[38] Okokpujie I. P., Okonkwo U. C., Fayomi O. S. I., Dirisu G. B. (2019). Data on Physicochemical Properties of Borehole Water and Surface Water Treated using Reverse Osmosis (RO) and Ultra-Violet (UV) Radiation Water Treatment Techniques. Chemical Data Collections 20(2019) 100207, 1-17.

[39] Da Silva, Wilton Pereira, Cleide MDPS e Silva, Fernando JA Gama, and Josivanda Palmeira Gomes. Mathematical models to describe thin-layer drying and to determine drying rate of whole bananas. Journal of the Saudi Society of Agricultural Sciences, 2014. 13, no. 1: 67-74.

[40] Nkolo M., Y., J. Noah Ngamveng, and S. Bardet, Effect of enthalpy-entropy compensation during sorption of water vapour in tropical woods: The case of Bubinga (Guibourtia Tessmanii J. Léonard; G. Pellegriniana JL). Thermochimica Acta, 2008. 468(1): p. 1-5.

[41] Okonkwo U. C., Abdulraheem A. A., Okokpujie I. P., Olaitan S. A. (2017). Development of a Rocket Stove Using Woodash as Insulator. Journal of Engineering and Applied Sciences. 10(2016-2017) 161 - 174.

[42] Corrêa, P.C., G.H.H. Oliveira, F.M. Botelho, A.L.D. Goneli, and F.M. Carvalho, Modelagem matemática e determinação das propriedades termodinâmicas do café (Coffea arabica L.) durante o processo de secagem. Revista Ceres, 2010. 57: p. 595-601.

[43] Martins, E.A., E.Z. Lage, A.L. Goneli, C.P. Hartmann, and J.G. Lopes, Cinética de secagem de folhas de timbó (Serjania marginata Casar). Revista Brasileira de Engenharia Agrícola e Ambiental, 2015. 19: p. 238-244.